Physics and Technology

EMITTERS

Materials

Infrared emitting diodes (IREDs) can be produced from a range of different III-V compounds. Unlike the elemental semiconductor silicon, compound III-V semiconductors consist of two or more different elements of group three (e.g., Al, Ga, In) and five (e.g., P, As) of periodic table. The bandgap energies of these compounds vary between 0.18 eV and 3.4 eV. However, the IREDs considered here emit in the near infrared spectral range between 800 nm and 1000 nm, and, therefore, the selection of materials is limited to GaAs and mixed crystal $Ga_{1-X}Al_XAs$, $0 \leq X \leq 0.8$, made from pure compounds GaAs and AlAs.

Infrared radiation is produced by the radiative recombination of electrons and holes from the conduction and valence bands. Emitted photon energy, therefore, corresponds closely to bandgap energy E_g. The emission wavelength can be calculated according to the formula λ (μm) = 1.240/Eg (eV). Internal efficiency depends on band structure, doping material and doping level. Direct bandgap materials offer high efficiencies, because no phonons are needed for recombination of electrons and holes. GaAs is a direct gap material and $Ga_{1-X}Al_XAs$ is direct up to X = 0.44. Doping species Si provides the best efficiencies and the shifts emission wavelength below the bandgap energy into the infrared spectral range by about 50 nm typically. Charge carriers are injected into the material via pn junctions. Junctions of high injection efficiency are readily formed in GaAs and $Ga_{1-X}Al_XAs$. P-type conductivity can be obtained with metals of valency two, such as Zn and Mg, and n-type conductivity with elements of valency six, such as S, Se and Te. However, silicon of valency four can occupy sites of III-valence and V-valence atoms, and, therefore, acts as donor and as acceptor. Conductivity type depends primarily on material growth temperature. By employing exact temperature control, pn junctions can be grown with the same doping species Si on both sides of the junction. Ge, on the other hand, also has a valency of four, but occupies group V sites at high temperatures i.e., p-type.

Only mono crystalline material is used for IRED production. In the mixed crystal system $Ga_{1-X}Al_XAs$, $0 \leq X \leq 0.8$, lattice constant varies only by about 1.5 x 10^{-3}. Therefore, mono crystalline layered structures of different $G_{a1-X}Al_XAs$ compositions can be produced with extremely high structural quality. These structures are useful because the bandgap can be shifted from 1.40 eV (GaAs) to values beyond 2.1 eV which enables transparent windows and heterogeneous structures to be fabricated. Transparent windows are another suitable means to increase efficiency, and heterogeneous structures can provide shorter switching times and higher efficiency. Such structures are termed single hetero (SH) or double hetero structures (DH). DH structures consist normally of two layers that confine a layer with a much smaller bandgap.

The best production method for all materials needed is liquid phase epitaxy (LPE). This method uses Ga-solutions containing As, possibly Al, and a doping substance. The solution is saturated at a high temperature, typically 900 °C, and GaAs substrates are dipped into the liquid. The solubility of As and Al decreases with decreasing temperature. In this way epitaxial layers can be grown by slow cooling of the solution. Several layers differing in composition may be obtained using different solutions one after another, as needed e.g. for DHs.

In liquid phase epitaxial reactors, production quantities of up to 50 wafers, depending on type of structure required, can be handled.

IRED CHIPS AND CHARACTERISTICS

In the past IRED chips are made only from GaAs. The structure of the chip is displayed in figure 1.

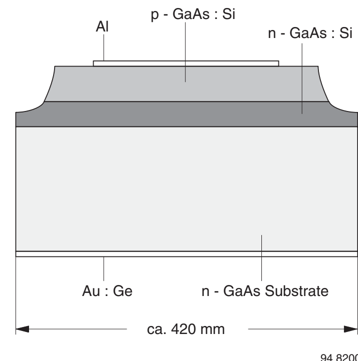

Fig. 1

On an n-type substrate, two Si-doped layers are grown by liquid phase epitaxy from the same solution producing an emission wavelength of 950 nm. Growth starts as n-type at high temperature and becomes p-type below about 820 °C. A structured Al-contact on p-side and a large area Au:Ge contact on back side provide a very low series resistance.

The angular distribution of emitted radiation is displayed in figure 2.

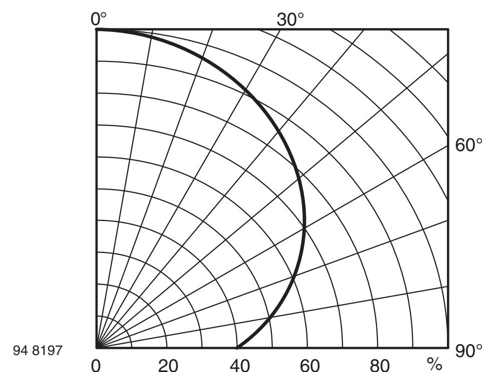

Fig. 2

For technical questions, contact: emittertechsupport@vishay.com
THIS DOCUMENT IS SUBJECT TO CHANGE WITHOUT NOTICE. THE PRODUCTS DESCRIBED HEREIN AND THIS DOCUMENT ARE SUBJECT TO SPECIFIC DISCLAIMERS, SET FORTH AT www.vishay.com/doc?91000

The package of the chip has to provide good collection efficiency of radiation emitted sideways, and has to diminish the refractive index step between the chip (n = 3.6) and the air (n = 1.0) with an epoxy of refractive index of 1.55. In this way, the output power of chip is increased by a factor of 3.5 for the assembled device.

The chip described is the most cost-efficient one. Its forward voltage at I_F = 1.5 A has the lowest possible value. Total series resistance is typically only 0.60 Ω; output power and linearity (defined as optical output power increase, divided by current increase between 0.1 A and 1.5 A) are high. Relevant data on chip and a typical assembled device are given in table 1.

The technology used for a chip emitting at 880 nm eliminates the absorbing substrate and uses only a thick epitaxial layer. The chip is shown in figure 3.

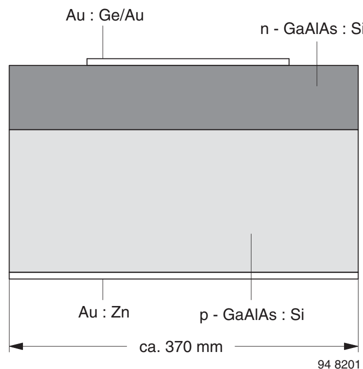

Fig. 3

Originally, the GaAs substrate was adjacent to the n-side. Growth of $Ga_{0.7}Al_{0.3}As$ started as n-type and became p-type - as in the first case - through the specific properties of the doping material Si. A characteristic feature of the Ga-Al-As phase system causes the Al-content of growing epitaxial layer to decrease. This causes the Al-concentration at the junction to drop to 8 % ($Ga_{0.92}Al_{0.08}As$), producing an emission wavelength of 880 nm. During further growth the Al-content approaches zero. The gradient of the Al-content and correlated gradient of bandgap energy produce an emission band of a relatively large half width. The transparency of the large bandgap material results in a high external efficiency on this type of chip.

The chip is mounted n-side up, and the front side metallization is Au:Ge/Au, whereas the reverse side metallization is Au:Zn.

The angular distribution of the emitted radiation is displayed in figure 4.

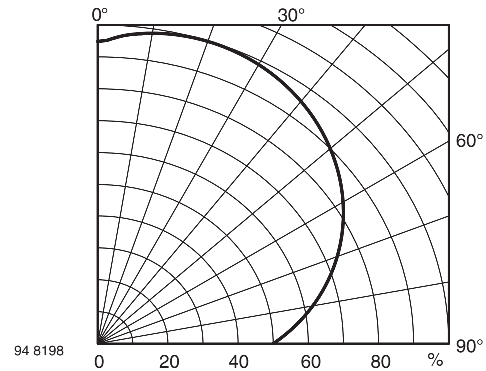

Fig. 4

Due to its shorter wavelength, $Ga_{1-X}Al_XAs$ chip described above offers specific advantages in combination with a Si detector. Integrated opto ICs, like amplifiers or Schmitt Triggers, have higher sensitivities at shorter wavelengths. Similarly, phototransistors are also more sensitive. Finally, the frequency bandwidth of pin diodes is higher at shorter wavelengths. This chip also has the advantage of having high linearity up to and beyond 1.5 A. The forward voltage, however, is higher than the voltage of a GaAs chip. Table 2 (see “Symbols and Terminology”) provides more data on the chip.

A technology combining some of the advantages of the two technologies described above is summarized in figure 5.

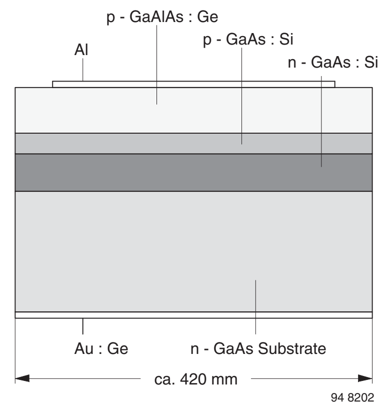

Fig. 5

Starting an with n-type substrate, n- and p-type GaAs layers are grown in a similar way to the epitaxy of a standard GaAs:Si diode. After this, a highly transparent window layer of $Ga_{1-X}Al_XAs$, doped p-type is grown. The upper contact to the p-side is made of Al and the rear side contact is Au:Ge. The angular distribution of emitted radiation is shown in figure 6.

For technical questions, contact: emittertechsupport@vishay.com
THIS DOCUMENT IS SUBJECT TO CHANGE WITHOUT NOTICE. THE PRODUCTS DESCRIBED HEREIN AND THIS DOCUMENT ARE SUBJECT TO SPECIFIC DISCLAIMERS, SET FORTH AT www.vishay.com/doc?91000

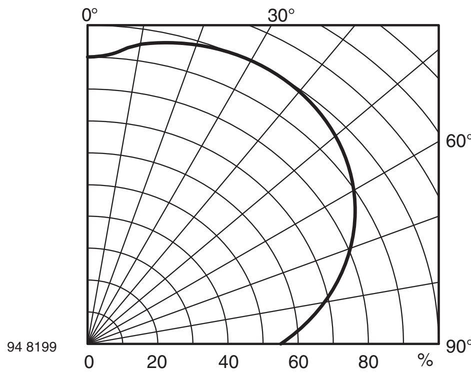

Fig. 6

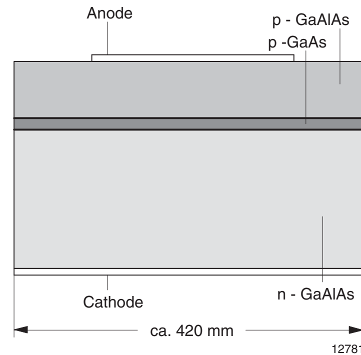

Fig. 7

This chip type combines a relatively low forward voltage with a high electro-optical efficiency, offering an optimized combination of the advantageous characteristics of the two other chips. Refer again to table 2 (see "Symbols and Terminology") for more details.

As mentioned in the previous section, double heterostructures (DH) provide even higher efficiencies and faster switching times. A schematic representation of such a chip is shown in figure 7.

The active layer is depicted as the thin layer between the p- and n- type $Ga_{1-X}Al_XAs$ confinement layers.

The contacts are dependent on the polarity of the chip. If p is up, then the p-side contact is Al and the back side Au:Ge; if n is up, then this side has an Au:Ge contact and the back side Au:Zn.Two such chips that are also very suitable for IrDA applications are given in table 1.

BULK AND SURFACE EMITTER TECHNOLOGY

A more recent technology, the surface emitter chip technology, involves bonding the Infrared emitting diode structure to a metalized conducting carrier substrate, after which the substrate, which was originally used for the epitaxial growth of the Infrared emitting crystal layers, is chemically removed. The layer structure of these diodes is extremely thin which has the favorable consequence that side wall emission is minimized.

The layers of the surface emitter IRED structures are deposited by metal-organic chemical vapor deposition (MOVPE) on suitable substrates. The active region consists of a multiple-quantum-well (MQW) or a DH structure. MQW active regions for Infrared emitting diodes contain typically one or more 5 nm thick InGaAs quantum wells which are separated by 15 nm thick GaAlAsP barriers.

High electro-optical efficiencies are achieved by the implementation of a metallic mirror on the back side of the layer structure which redirects the incident radiation effectively towards the top surface as well as a treatment of the top surface to increase the extraction efficiency. As sidewall emission is negligible radiance scales with chip area and large devices can be realized without significant increase of reabsorption losses.

In order to provide a good current spreading and a uniform current distribution surface emitter diodes are grown n-side up. Both contacts, the structured top electrode to the n-side and the large area back side contact, are made of gold.

The angular distribution of the emitted radiation corresponds nearly perfectly to the lambertian emission pattern of point sources $I_0 = I(\phi) \times \cos \phi$ and enables an efficient coupling of the output power into optical systems.

Exemplary data on chip and assembled device are given in table 1.

A further Infrared emitter chip technology, which makes use of metal organic chemical vapor deposition, is the bulk emitter chip technology. On an n-type GaAs substrate a MQW structure similar to the one described above is grown producing an emission wavelength of 940 nm. As the substrate is transparent at this wavelength the bulk emitter technology offers the high efficiencies of double hetero structures in combination with exceptional low forward voltages and very fast response times. With these favorable characteristics bulk emitter chips can substitute conventional GaAlAs/GaAs chips in many technical applications. As electrode material for the top p-type contact Al or Au are in use, whereas the back side contact consists of an Au alloy. The angular distribution of the emitted radiation resembles the one shown in figure 6. Relevant chip and device data are given in table 1.

For technical questions, contact: emittertechsupport@vishay.com
THIS DOCUMENT IS SUBJECT TO CHANGE WITHOUT NOTICE. THE PRODUCTS DESCRIBED HEREIN AND THIS DOCUMENT ARE SUBJECT TO SPECIFIC DISCLAIMERS, SET FORTH AT www.vishay.com/doc?91000

TABLE 1: CHARACTERISTICS DATA OF IRED CHIPS

TECHNOLOGY	TYPICAL CHIP DATA				TYPICAL DEVICE	TYPICAL DEVICE DATA			
	Φ_e at 0.1 A (mW)	λ_p (nm)	$\Delta\lambda$ (nm)	POLARITY		Φ_e at 0.1 A (mW)	V_F at 0.1 A (V)	V_F at 1.0 A (V)	t_r at 0.1 A (ns)
GaAs	7.7	950	50	p up	TSUS540.	20	1.3	2.1	800
GaAlAs	12.8	875	80	n up	TSHA550.	27	1.5	3.4	600
GaAlAs (DDH)	20	890	40	p up	TSHF5410	45	1.5	2.3	30
GaAlAs (DDH)	26	870	40	p up	TSFF5410	50	1.5	2.3	15
Bulk Emitter	21	940	30	p up	VSLB3940	40	1.35	2.1	15
GaAlAs MQW	22	940	30	p up	TSAL6200	40	1.35	2.2	15
Surface Emitter	30	850	25	n up	VSLY5850	55	1.65	2.9	10

UV, VISIBLE, AND NEAR IR SILICON PHOTODETECTORS

(adapted from ”Sensors, Vol 6, Optical Sensors, Chapt. 8, VCH - Verlag, Weinheim 1991”)

Silicon Photodiodes (PN and PIN Diodes)

The physics of silicon detector diodes

Absorption of radiation is caused by the interaction of photons and charge carriers inside a material. The different energy levels allowed and the band structure determine the likelihood of interaction and, therefore, the absorption characteristics of the semiconductors. The long wavelength cutoff of the absorption is given by the bandgap energy. The slope of the absorption curve depends on the physics of interaction and is much weaker for silicon than for most other semiconducting materials. This results in a strong wavelength-dependent penetration depth which is shown in figure 8. (The penetration depth is defined as that depth where 1/e of the incident radiation is absorbed.)

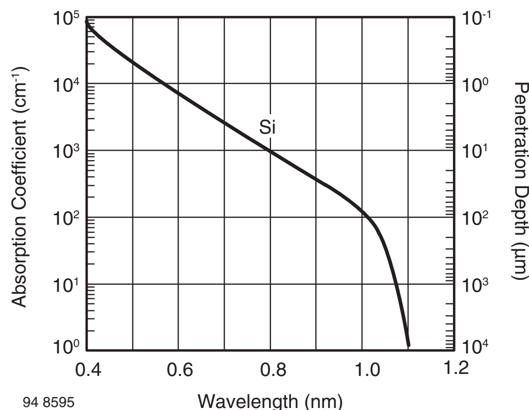

Fig. 8 - Absorption and Penetration Depth of Optical Radiation in Silicon

Depending on the wavelength, the penetration depth varies from tenths of a micron at 400 nm (blue) to more than 100 µm at 1 µm (IR). For detectors to be effective, an interaction length of at least twice the penetration depth should be realized (equivalent to $1/e^2$ = 86 % absorbed radiation). In the pn diode, generated carriers are collected by the electrical field of the pn junction. Effects in the vicinity of a pn junction are shown in figure 9 for various types and operating modes of the pn diode. Incident radiation generates mobile minority carriers - electrons on the p-side, holes on the n-side. In the short circuit mode shown in figure 9 (top), the carriers drift under the field of the built-in potential of the pn junction. Other carriers diffuse inside the field-free semiconductor along a concentration gradient, which results in an electrical current through the applied load, or without load, in an external voltage, open circuit voltage, V_{OC}, at contact terminals. Bending of the energy bands near the surface is caused by surface states. An equilibrium is established between generation, recombination of carriers, and current flow through the load.

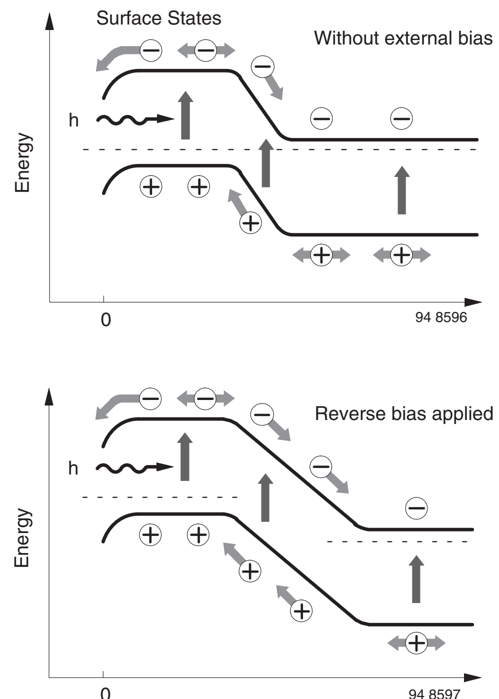

Fig. 9 - Generation-Recombination Effects in the Vicinity of a PN Junction
Top: Short Circuit Mode, Bottom: Reverse Biased

For technical questions, contact: emittertechsupport@vishay.com
THIS DOCUMENT IS SUBJECT TO CHANGE WITHOUT NOTICE. THE PRODUCTS DESCRIBED HEREIN AND THIS DOCUMENT ARE SUBJECT TO SPECIFIC DISCLAIMERS, SET FORTH AT www.vishay.com/doc?91000

Recombination takes place inside the bulk material with technology- and process-dependent time constants which are very small near the contacts and surfaces of the device. For short wavelengths with very small penetration depths, carrier recombination is the efficiency limiting process. To achieve high efficiencies, as many carriers as possible should be separated by the electrical field inside the space charge region. This is a very fast process, much faster than typical recombination times (for data, see chapter 'Operating modes and circuits').

The width, W, of the space charge is a function of doping the concentration N_B and applied voltage V:

$$W = \sqrt{\frac{2 \times \varepsilon_S \times \varepsilon_o \times (V_{bi} + V)}{q \times N_B}} \quad (1)$$

(for a one-sided abrupt junction), where V_{bi} is built-in voltage, ε_s dielectric constant of Si, ε_o vacuum dielectric constant and q is electronic charge. The diode's capacitance (which can be speed limiting) is also a function of the space charge width and applied voltage. It is given by

$$C = \frac{\varepsilon_S \times \varepsilon_o \times A}{W} \quad (2)$$

where A is the area of the diode. An externally applied bias will increase the space charge width (see figure 8) with the result that a larger number of carriers are generated inside this zone which can be flushed out very fast with high efficiency under the applied field. From equation (1), it is evident that the space charge width is a function of the doping concentration N_B. Diodes with a so-called pin structure show according to equation (1) a wide space charge width where i stands for intrinsic, low doped. This zone is also sometimes nominated as n or p rather than low doped n, n- or p, p-zone indicating the very low doping. Per equation (2), the junction capacitance C, is low due to the large space charge region of PIN photodiodes. These photodiodes are mostly used in applications requiring high speed.

Figure 10 shows a cross section of PIN photodiodes and PN diodes. The space charge width of the PIN photodiodes (bottom) with a doping level ($n = N_B$) as low as $N_B = 5 \times 1011\ cm^{-3}$ is about 80 µm wide for a 2.5 V bias in comparison with a pn diode with a doping (n) of $N_B = 5 \times 1015\ cm^{-3}$ with only 0.8 mm.

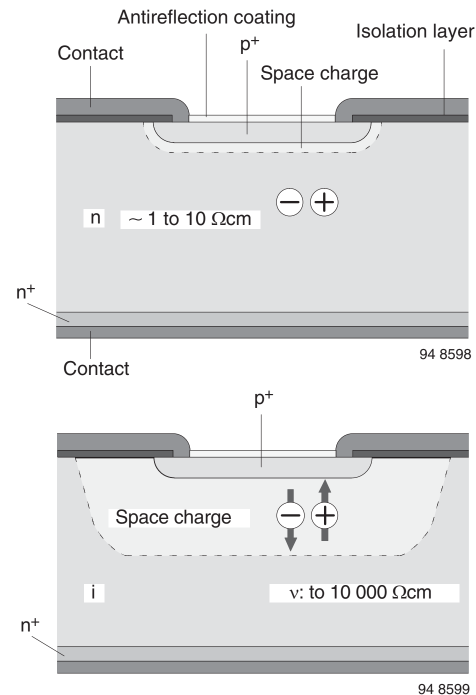

Fig. 10 - Comparison of PN Diode (Top) and PIN Photodiode (Bottom)

PROPERTIES OF SILICON PHOTODIODES

I-V Characteristics of illuminated pn junction

The cross section and I-V-characteristics of a photodiode are shown in figure 11 and 12. The characteristic of the illuminated diode is identical to the characteristic of a standard rectifier diode. The relationship between current, I, and voltage, V, is given by

$$I = I_S \times \left(\frac{\exp V}{V_T - 1}\right) \quad (3)$$

with $V_T = kT/q$

$k = 1.38 \times 10^{-23}\ JK^{-1}$, Boltzmann constant

$q = 1.6 \times 10^{-19}$ As, electronic charge.

I_S, the dark-reverse saturation current, is a material- and technology-dependent quantity. The value is influenced by the doping concentrations at pn junction, by carrier lifetime, and especially by temperature. It shows a strongly exponential temperature dependence and doubles every 8 °C.

For technical questions, contact: emittertechsupport@vishay.com
THIS DOCUMENT IS SUBJECT TO CHANGE WITHOUT NOTICE. THE PRODUCTS DESCRIBED HEREIN AND THIS DOCUMENT ARE SUBJECT TO SPECIFIC DISCLAIMERS, SET FORTH AT www.vishay.com/doc?91000

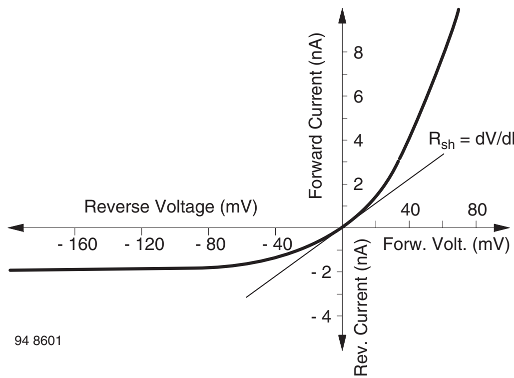

Fig. 11 - Measured I-V-Characteristics of an Si Photodiode in the Vicinity of the Origin

The typical dark currents of Si photodiodes are dependent on size and technology and range from less than picoamps up to tens of nanoamps at room temperature conditions. As noise generators, dark current I_{r0} and the resistance R_{sh} (defined and measured at a voltage of 10 mV forward or reverse, or peak-to-peak) are limiting quantities when detecting very small signals.

The photodiode exposed to optical radiation generates a photocurrent I_r exactly proportional to incident radiant power Φ_e.

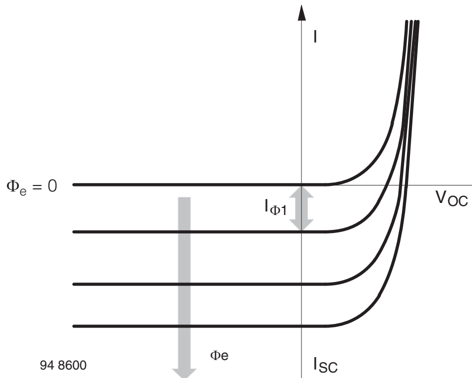

Fig. 12 - I-V-Characteristics of an Si Photodiode under Illumination. Parameter: Incident Radiant Flux

The quotient of both is spectral responsibility s(λ),

$$S(\lambda) = \frac{I_r}{\phi_e[A/W]} \tag{4}$$

The characteristic of the irradiated photodiode is then given by

$$I = I_S \times \left(\frac{\exp V}{V_T - 1}\right) - S(\lambda) \times \phi_e \tag{5}$$

and in case V ≈ 0, zero or reverse bias we find,

$$I = -I_S - S(\lambda) \times \phi_e \tag{6}$$

Dependent on load resistance, R_L, and applied bias, different operating modes can be distinguished. An unbiased diode operates in photovoltaic mode. Under short circuit conditions (load R_L = 0 Ω), short circuit current, I_{SC} flows into the load. When R_L increases to infinity, the output voltage of the diode rises to the open circuit voltage, V_{OC}, given by

$$V_{OC} = V_T \times \left(\frac{S(\lambda) \times \phi_e}{I_S + 1}\right) \tag{7}$$

Because of this logarithmic behavior, the open circuit voltage is sometimes used for optical light meters in photographic applications. The open circuit voltage shows a strong temperature dependence with a negative temperature coefficient. The reason for this is the exponential temperature coefficient of the dark reverse saturation current I_S. For precise light measurement, a temperature control of the photodiode is employed. Precise linear optical power measurements require small voltages at the load, typically smaller than about 5 % of the corresponding open circuit voltage. For less precise measurements, an output voltage of half the open circuit voltage can be allowed. The most important disadvantage of operating in photovoltaic mode is the relatively large response time. For faster response, it is necessary to implement an additional voltage source reverse-biasing the photodiode. This mode of operation is termed photoconductive mode. In this mode, the lowest detectable power is limited by the shot noise of the dark current, I_S, while in photovoltaic mode, the thermal (Johnson) noise of shunt resistance, R_{sh}, is the limiting quantity.

SPECIAL RESPONSITIVITY

Efficiency of Si photodiodes:

The spectral responsivity, s_λ, is given as the number of generated charge carriers (η x N) per incident photons N of energy h x ν (η is percent efficiency, h is the Plancks constant, and ν is the radiation frequency). Each photon will generate one charge carrier at the most. The photocurrent I_{re} is then given as

$$I_{re} = \eta \times N \times q \tag{8}$$

$$S(\lambda) = \left(\frac{I_{re}}{\phi_e}\right) = \frac{\eta \times N \times q}{h \times \nu \times N} = \frac{\eta \times q}{h \times \nu} \tag{9}$$

$$S(\lambda) = \frac{\lambda(\mu m)}{1.24}[A/W]$$

At fixed efficiency, a linear relationship between wavelength and spectral responsivity is valid.

Figure 8 shows that the semiconductors absorb radiation similar to a cut-off filter. At wavelengths smaller than the cut-off wavelength, the incident radiation is absorbed. At larger wavelengths the radiation passes through the material without interaction. The cut-off wavelength corresponds to the bandgap of the material. As long as the energy of the photon is larger than the bandgap, carriers can be generated by absorption of photons, provided that the material is thick enough to propagate photon-carrier interaction. Bearing in mind that the energy of photons decreases with increasing wavelength, we can see, that the curve of the spectral responsivity vs. wavelength in ideal

For technical questions, contact: emittertechsupport@vishay.com
THIS DOCUMENT IS SUBJECT TO CHANGE WITHOUT NOTICE. THE PRODUCTS DESCRIBED HEREIN AND THIS DOCUMENT ARE SUBJECT TO SPECIFIC DISCLAIMERS, SET FORTH AT www.vishay.com/doc?91000

case (100 % efficiency) will have a triangular shape (see figure 13). For silicon photodetectors, the cut-off wavelength is near 1100 nm.

In most applications, it is not necessary to detect radiation with wavelengths larger than 1000 nm. Therefore, designers use a typical chip thickness of 200 μm to 300 μm, which results in reduced sensitivity at wavelengths larger than 950 nm. With a typical chip thickness of 250 μm, an efficiency of about 35 % at 1060 nm is achieved. At shorter wavelengths (blue-near UV, 500 nm to 300 nm) sensitivity is limited by recombination effects near the surface of the semiconductor. A reduction in efficiency starts near 500 nm and increases as the wavelength decreases. Standard detectors designed for visible and near IR radiation may have poor UV/blue sensitivity and poor UV stability. Well designed sensors for wavelengths of 300 nm to 400 nm can operate with fairly high efficiencies. At shorter wavelengths (< 300 nm), efficiency decreases strongly.

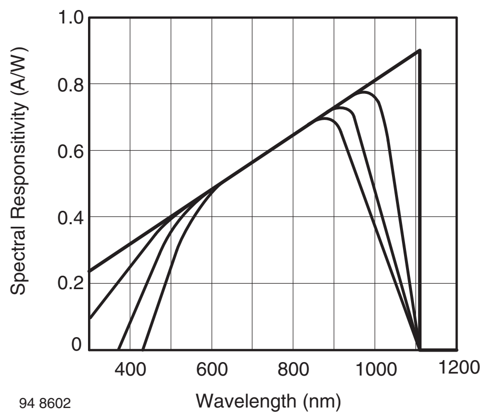

Fig. 13 - Spectral Responsivity as a Function of Wavelength of a Si Photodetector Diode, Ideal and Typical Values

Temperature dependence of spectral responsivity

The efficiency of carrier generation by absorption and the loss of carriers by recombination are the factors which influence spectral responsivity. The absorption coefficient increases with temperature. The radiation of the long wavelength is therefore more efficiently absorbed inside the bulk and results in increased response. For shorter wavelengths (< 600 nm), reduced efficiency is observed with increasing temperature because of increased recombination rates near the surface. These effects are strongly dependent on technological parameters and therefore cannot be generalized to the behavior at longer wavelengths.

Uniformity of spectral responsivity

Inside the technologically defined active area of photodiodes, spectral responsivity shows a variation of sensitivity on the order of < 1 %. Outside the defined active area, and especially at lateral edges of the chips, local spectral response is sensitive to applied reverse voltage. Additionally, this effect depends on wavelength. Therefore, the relation between power (W) related spectral responsivity, s_λ (A/W), and power density (W/cm^2) related spectral responsivity, s_λ [A/(W/cm^2)] is not a constant. Rather, this relation is a function of wavelength and reverse bias

Stability of spectral responsivity

Si detectors for wavelengths between 500 nm and 800 nm appear to be stable over very long periods of time. In the literature concerned here, remarks can be found on instabilities of detectors in blue, UV, and near IR under certain conditions. Thermal cycling reversed the degradation effects.

Surface effects and contamination are possible causes but are technologically well controlled.

Angular dependence of responsivity

The angular response of Si photodiodes is given by the optical laws of reflection. The angular response of a detector is shown in figure 14.

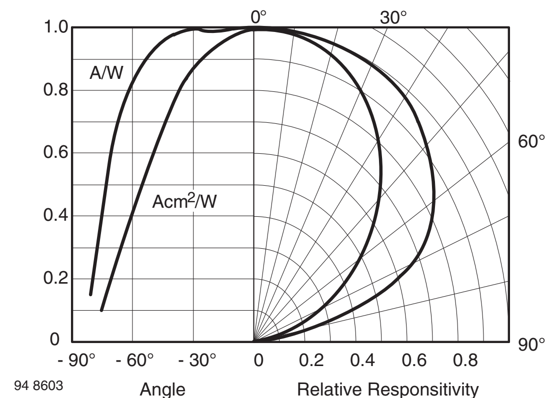

Fig. 14 - Responsivity of Si Photodiodes as a Function of the Angle of Incidence

Semiconductor surfaces are covered with quarter wavelength anti-reflection coatings. Encapsulation is performed with uncoated glass or sapphire windows.

The bare silicon response can be altered by optical imaging devices such as lenses. In this way, nearly every arbitrary angular response can be achieved.

Dynamic Properties of Si Photodiodes

Si photodiodes are available in many different variations. The design of diodes can be tailored to meet special needs. Si photodiodes may be designed for maximum efficiency at given wavelengths, for very low leakage currents, or for high speed. The design of a photodiode is nearly always a compromise between various aspects of a specification.

Inside the absorbing material of the diode, photons can be absorbed in different regions. For example at the top of a p^+n^--diode there is a highly doped layer of p^+ - Si. Radiation of shorter wavelengths will be effectively absorbed, but for larger wavelengths only a small amount is absorbed. In the vicinity of the pn junction, there is the space charge region, where most of the photons should generate carriers. An electric field accelerates the generated carrier in this part of the detector to a high drift velocity. Carriers which are not

For technical questions, contact: emittertechsupport@vishay.com
THIS DOCUMENT IS SUBJECT TO CHANGE WITHOUT NOTICE. THE PRODUCTS DESCRIBED HEREIN AND THIS DOCUMENT ARE SUBJECT TO SPECIFIC DISCLAIMERS, SET FORTH AT www.vishay.com/doc?91000

absorbed in these regions penetrate into field-free region where the motion of the generated carriers fluctuates by a slow diffusion process.

The dynamic response of the detector is composed of different processes which transport carriers to contacts. The dynamic response of photodiodes is influenced by three fundamental effects:

- Drift of carriers in an electric field
- Diffusion of carriers
- Capacitance x load resistance

Carrier drift in the space charge region occurs rapidly with very small time constants. Typically, transit times in an electric field of 0.6 V/μm are on the order of 16 ps/μm and 50 ps/μm for electrons and holes, respectively. At (maximum) saturation velocity, the transit time is on the order of 10 ps/μm for electrons in p-material. With a 10 μm drift region, traveling times of 100 ps can be expected. Response time is a function of the distribution of the generated carriers and is therefore dependent on wavelength.

The diffusion of the carriers is a very slow process. Time constants are on the order of some ms. The typical pulse response of the detectors is dominated by these two processes. Obviously, carriers should be absorbed in large space charge regions with high internal electrical fields. This requires material with an adequate low doping level.

Furthermore, a reverse bias of rather large voltage is useful. Radiation of shorter wavelength is absorbed in smaller penetration depths. At wavelengths shorter than 600 nm, decreasing wavelength leads to an absorption in the diffused top layer. The movement of carriers in this region is also diffusion limited. Because of the small carrier lifetimes, the time constants are not as large as in homogeneous substrate material.

Finally, capacitive loading of output in combination with load resistance limits frequency response.

PROPERTIES OF SILICON PHOTOTRANSISTORS

The phototransistor is equivalent to a photodiode in conjunction with a bipolar transistor amplifier (figure 15). Typically, the current amplification, B, is between 100 and 1000 depending on type and application. The active area of phototransistor is usually about 0.5 x 0.5 mm^2.

The data of spectral responsivity are equivalent to those of photodiodes, but must be multiplied by the factor current amplification, B.

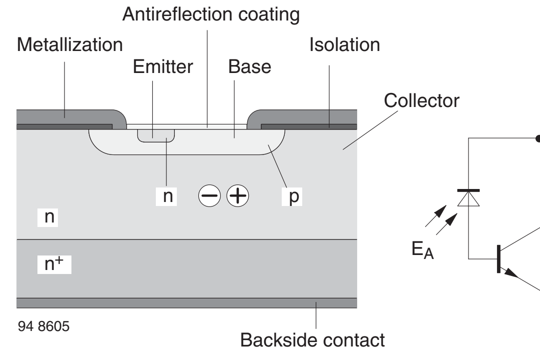

Fig. 15 - Phototransistor, Cross Section and Equivalent Circuit

The switching times of phototransistors are dependent on current amplification and load resistance and are between 30 ms and 1 ms. The resulting cut-off frequencies are a few hundred kHz.

The transit times, t_r and t_f, are given by

$$t_{r,\,f} = \sqrt{\left(\frac{1}{2 \times f_t^2}\right)^2 + b \times (RC_B \times V)^2} \qquad (10)$$

f_t: Transit frequency

R: Load resistance, 1.6

C_B: Base-collector capacitance, b = 4 to 5

V: Amplification

Phototransistors are most frequently applied in transmissive and reflective optical sensors.

For technical questions, contact: emittertechsupport@vishay.com
THIS DOCUMENT IS SUBJECT TO CHANGE WITHOUT NOTICE. THE PRODUCTS DESCRIBED HEREIN AND THIS DOCUMENT ARE SUBJECT TO SPECIFIC DISCLAIMERS, SET FORTH AT www.vishay.com/doc?91000